Supplement of Atmos. Chem. Phys., 25, 1545–1567, 2025
https://doi.org/10.5194/acp-25-1545-2025-supplement

Atmospheric Chemistry and Physics
Open Access
EGU

Supplement of

Biomass burning emission analysis based on MODIS aerosol optical depth and AeroCom multi-model simulations: implications for model constraints and emission inventories

Mariya Petrenko et al.

Correspondence to: Ralph Kahn (ralph.kahn@lasp.colorado.edu)

Supplement S1. On the use of case box as a unit of spatial and temporal comparison

Observations and model output need to be brought to a common temporal and spatial resolution for comparison. The data are either re-gridded or subset to satisfy this requirement. Since we are using an original approach of comparing model observations to a set of satellite snapshots, we've had many internal deliberations to arrive at the case box as the unit of comparison in this study. Here are some of our considerations:

- The boxes are of different sizes. One of the main criteria for outlining the boxes was that they were at least a 100 km in one linear dimension – so that they are big enough to be resolved by a model with about a 1-degree resolution (main criteria are summarized in section 2.3). Most of boxes are larger than this.

- All boxes are near-source. (Fire hot spots must be detected in the MO/YD14 product, and an associated AOD pattern must be observed in the MODIS visible image.) Having smoke cases tied closely in space and time to the actual fire allows for meaningful analysis when the case sizes vary. If the case box encloses the actual smoke plume, then we are directly investigating the model BB processes. For example, for small cases, the emissions in the box will be smaller, and the AOD of the plume will depend on the model dynamics, deposition, chemistry, optical algorithm, as appropriate. For larger cases, the smoke plume associated with the fire will be defined by the same model processes but over a larger burning area, or alternatively, more fires will be included in the box. (There will be more particles in the box from multiple sources, but this plume will also be bigger, so, consistently, AOD will be averaged over the larger box.)

  This near-source approach also calls for model sampling closest to satellite observations. We took AOD from the daily mean of the UTC date of satellite observation (we also did not notice a significant difference between sampling the closest 3-hr model output vs daily output), and other variables (loading, deposition, extinction) from the monthly mean, because that was the model output available.

- Regarding the resolution of the models and satellite product. Participating models have horizontal resolutions from 0.5 x 0.625 to 4 x 5 degrees. With satellite product at 10 km horizontal resolution, we needed some common resolution to compare them. Averaging all these different products over the case box seems reasonable, because it would smooth any possible higher peaks in the finer-resolution products, and distributes the variable of interest over the same area. Also, given different sizes of the case boxes, this approach includes the variable information relevant to every fire case, regardless of its size. So, to get the case average, we average the values of all grid boxes, the centers of which fall within the geographic boundaries of the case rectangle, whatever the original resolution of the grid we are averaging. (We did try to calculate case box averages, taking into consideration partial inclusion of the model grid box or satellite pixel, but it did not make much of a difference, and having the center of the model/satellite grid fall within the boundaries of the fire case is an approximation that includes a large enough portion of the grid to be averaged equally.)

Table S1 Sources of non-BB aerosol in the models and aerosol properties

MODEL	Anthropogenic emissions	Dust	Volcanic	Sea salt	Default model emission injection height
CAM5	SO_2, BC, and OC from fossil fuel and biofuel combustion: Aerocom2-ACCMIP (Lamarque et al., 2010)	Calculated using friction velocity, soil erodibility, soil moisture.	Non-eruptive volcanic SO2 emissions from AeroCOM (Dentener et al., 2006a)	Calculated using 10-m wind speed, sea surface temperature.	Anthrop. emissions: model surface layer. Energy and industry: 100-300 m above surface. BB: evenly distributed from 0 to 1 km.
ECMWF-IFS (CY45R1)	SO_2 , OC and BC from non BB source, from MACCity BB BC and OC: GFAS (Kaiser et al., 2012)	Calculated using surface topography, surface bareness, 10 m wind speed, and ground wetness (Ginoux et al., 2001). Updated with the use of wind gusts.	none	Calculated using 10-m wind speed (Monahan and O'Muircheartaigh, 1986; Morcrette et al., 2009)	BB: Daily injection heights computed by a Plume Rise Model (Paugam et al., 2015).
ECHAM6-SALSA (6.1)	SO_2, BC, and OC from fossil fuel and biofuel combustion: Aerocom2-ACCMIP (Lamarque et al., 2010)	Dust flux calculated on-line using10 m wind speeds, soil clay content and soil moisture from ECHAM6 (Bergman et al., 2012; Tegen et al., 2002)	Emissions from volcanic sources are based on GEIA inventory (Andres and Kasgnoc, 1998a)	Calculated using 10-m wind speed (Bergman et al., 2012)	Anthrop. emissions: model surface layer. Energy and industry: 100-300 m above surface. BB: prescribed ecosystem-specific emission profiles from 0 to 6 km. Volcanic: estimated from magnitude of eruption.
GEOS	SO2, NH3, BC, and OC from fossil fuel and biofuel combustion: HTAP2 dataset	5-bins calculated as a function of surface topography, surface bareness, 10 m wind speed, and ground wetness (Ginoux et al., 2001)	Global volcanic SO_2 emission inventory by Carn et al. (2017)	5-bins calculated based on met fields	BB emission: evenly distributed within the boundary layer. The rest (du, ss, anthropogenic: oc, bc, su) are injected in the lowest model layer. Volcanic SO_2 is distributed evenly within a layer defined in Carn's dataset (2017).
GEOS-CHEM (v9-02)	CO, NOx, and SO_2 from EDGAR v3.2-FT2000 (Olivier et al., 2005) NMVOCs: RETRO monthly global inventory for 2000 implemented after (Hu et al., 2015; Xiao et al.,	Fairlie et al. (2007)	Eruptive and non-eruptive volcanic SO_2 emissions for individual years are from the AEROCOM, (Fisher et al., 2011)	Jaegle et al. (2011)	Species are emitted in the lowest model level, and mixed homogeneously up to the mixing height recalculated in the model.

	2008; Yevich and Logan, 2003); Global anthrop. BC/OC: (Bond et al., 2007) GEIA ammonia emissions (Bouwman et al., 1997) the US NEI05, Canada (CAC), Mexico (BRAVO), Europe (EMEP), East Asian emissions from (Streets et al., 2006) and (Zhang et al., 2009) **Aircraft emissions** BC/OC, sulfur emissions calculated from fuel parameters (Stettler et al., 2011)				
GISS ModelE OMA	Emissions are taken from Lamarque et al. (2010)	Prognositc (friction velocity, soil erodibility, soil moisture)	Stratospheric AOD prescribed, continous SO_2 AeroCom	Prognostic (10-m wind speed, sea surface temperature)	Anthropogenic emissions from agricuture, domestic, transportation, waster, and shipping sectors are distributed to the model surface layer while those from energy and industry sectors are emitted at 100-300 m above surface ; fire emissions are evenly distributed in the boundary layer.
GISS ModelE MATRIX	Emissions are taken from Lamarque et al. (2010)	Prognositc (friction velocity, soil erodibility, soil moisture)	Stratospheric AOD prescribed, continous SO_2 AeroCom	Prognostic (10-m wind speed, sea surface temperature)	Anthropogenic emissions from agricuture, domestic, transportation, waster, and shipping sectors are distributed to the model surface layer while those from energy and industry sectors are emitted at 100-300 m above surface ; fire emissions are evenly distributed in the boundary layer.

GOCART (5 rev. 32)	SO_2, BC, and OC from fossil fuel and biofuel combustion: A2-ACCMIP dataset (Diehl et al., 2012)	Calculated using surface topography, surface bareness, 10-m wind speed, and ground wetness (Ginoux et al., 2001) Update including NDVI (Kim et al., 2013)	Volcanic SO_2 from (A2-MAP), + continuous volcanoes (Diehl et al., 2012)	Calculated based on met fields	BB: evenly distributed within the BL. Volcanic: estimated from magnitude of eruption and volcanic SO_2 index. The rest: injected in the lowest model layer.
HadGEM (3)	SO2, BC, and OC from fossil fuel and biofuel combustion are as prescribed as in IPCC AR5 / CMIP5 historical runs	Dust emissions are calculated as a function of bare soil cover, soil properties, soil moisture, and 10 m wind speed (Woodward, 2001)	Volcanic SO2 emissions are taken from Andres and Kasgnoc (1998b)	Sea salt emission calculated based on 10m wind speed (Gong, 2003; Spracklen et al., 2005)	BB emission are evenly distributed within the lowest 3km of the troposphere. The rest (du, ss, anthropogenic: oc, bc, su) are injected in the lowest model l ayer.
OsloCTM2	ECLIPSE V5 emissions for year 2010 (Stohl et al., 2015)	Interactive, (Grini et al., 2005)	Volcanic emissions from AEROCOM (Dentener et al., 2006b)	Interactive, (Grini et al., 2005)	Anthropogenic: distributed in the four lowest model layers dependent on emission sectors.
SPRINTARS	SO_2, BC, and OC from fossil fuel and biofuel combustion: HTAP2.	See Appendix A in (Takemura et al., 2009)	(Andres and Kasgnoc, 1998a)	See Appendix B in (Takemura et al., 2009)	BB emission are evenly distributed within the sigma level larger than 0.74. The rest: lowest model layer.

Table S2 Aerosol properties in the models

Model	Aerosol species considered in the model	Convection (dry and moist)	Boundary layer definition	Aerosol mass extinction efficiency at 550 nm	Aerosol refractive index at 550 nm	Hygroscopicity assumptions for BB-related species	BB-related aerosol aging assumptions
CAM5	du, ss, BC, primary organic matter (POM), secondary organic aerosol (SOA and precursor gases), sulfate (and its gaseous precursors SO_2 and DMS)	Park and Brethert on (2009); Zhang and McFarl ane (1995)	Diagnostic TKE-based 1st-order K diffusion scheme with entrainme nt parameteri zation (Park and Bretherton , 2009).	Wet RI in each mode is calculated based on the volume-weighted means of individual aerosol species. The wet surface mode radius of particles in the mode is calculated based on the Köhler theory. These two parameters are used to parameteri ze the optical properties of particles in the mode based on (Ghan and Zaveri, 2007).	(1.95,0.79i) for BC; OPAC (Hess et al., 1998) for other species.	0 for BC and 0.1 for POM; SO4=0.507	No aging assumptions applied; upon emission BC and POM are internally mixed with more hygroscopic species in the same accumulation mode, and thus subject to wet scavenging.
ECHAM6-SALSA (6.1)	du, ss, OC, BC, sulfate (and its gaseous precursors SO_2 and DMS)	Norden g (1994)	Equation 3, Stevens et al. (2013)	Look-up-tables based on mie calculation s for the extinction cross section, asymmetry factor, and single	Volume weighted means of individua l aerosol species (refractiv e indices are given by Bergman et al.	Hygroscopicity: ZSR method (Jacobson, 2005). BC completely insoluble, 15% of OC is soluble taking as an ideal solute, SO4 hygroscopicity is according to Jacobson (2005).	no ageing

				scattering albedo as a function of size parameter and refractive index.	(2012), Table 5.		
ECMWF-IFS (CY45R1)	du, ss, sulfate, OM, BC	Bulk mass scheme (Bechtold et al., 2014; Tiedtke, 1989)	Diagnostic following Troen and Mahrt (1986)	See Bozzo et al. (2020)	See Bozzo et al. (2020)	Considered only for optical properties (Rémy et al., 2019)	original 80% of BC and 50% of OC are hydrophyllic with e-folding time of 1.16 days
GEOS	du, ss, OC, BC, sulfate, nitrate, and ammonium	Dry: Resistent-in-series (Wesely, 1989); Moist: Relaxed Arakawa-Schubert convection scheme (Moorthi and Suarez, 1992)	Shear-based component of the turbulent kinetic energy (TKE) (McGrath-Spangler and Molod, 2014)	See Fig. 2 in Chin et al, (2002)	Table 2 from Chin et al. (2009)	Hygroscopic growth factors - see table 3 from Chin et al. (2002)	80% of BC and 50% of OC are hydrophyl. with e-folding time of 2.5 days
GEOS-CHEM (v9-02)	du, ss, OC, BC, sulfate, nitrates, ammonium, MSA	non-local PBL, (Holtslag and Boville, 1993). Moist: Relaxed Arakawa-Schubert convection scheme (Moorthi and Suarez, 1992)	Recalculated internally as a function of atmospheric stability (Lin et al., 2008; Lin and McElroy, 2010)	From GADS/OPAC. Data in m^2/g: sulfate, ammonium and nitrate 2.2; BC 8.0; OC 2.8; SS fine 2.4; SS coarse 0.9; dust from 3.1 to 0.16 from finer to coarser bin	From GADS/OPAC. Sulfate-ammonium-nitrate: $1.43 + 10^{-8}$ i; BC 1.75+0.45 i; OC 1.53+0.006 i; SS $1.5 + 10^{-8}$ i; dust 1.56 + 0.0014 i	Hygroscopicity factors are assigned in 7 RH bin for each species, and Mie scattering and absorption efficiencies recalculated at those bins, and the interpolated at ambient RH online.	Primary hydrophobic fraction of carbonaceous aerosol is converted to hydrofilic with an e-folding time of 1.2 days

GISS ModelE MATRIX	16 mixing state classes (for definition see (Bauer et al., 2008) containing: sulfate,nitrate,amminum,organics,BC,sea salt, mineral dust and aerosol water.	Schmidt et al. (2014) and references therein	Dynamic PBL		Sulfate (1.528-1.e-7i), nitrate (1.528-1.e- 7i), OC (1.527-0.014i), BC (1.85-0.71i), sea salt (1.45-0.i), dust (1.564-0.002i) and water (1.334-3.91e-8i)See Bauer et al 2010	Prognostic, determined by mixing state	
GISS ModelE OMA	du, su coated dust, nitrate coated dust, ss, BC, POM, SOA and precuror gases, sulfate (and its gaseous precursors SO2 and DMS), ammonium, nitrate, MSA	Schmidt et al., 2014 (and references therein)	Dynamic PBL		Sulfate (1.528-1.e-7i), nitrate (1.528-1.e- 7i), OC (1.527-0.014i), BC (1.85-0.71i), sea salt (1.45-0.i), dust (1.564-0.002i)	80% solubility assumed	No aging
GOCART (5 rev. 32)	du, ss, OC, BC, sulfate (and its gaseous precursors SO_2 and DMS)		provided by GEOS5	See Fig. 2 in Chin et al, (2002)	Table 2 from (Chin et al., 2009)	Hygroscopic growth factors - see table 3 below (Chin et al., 2002)	80% of BC and 50% of OC are hydrophyl. with e-folding time of 2 days
HadGEM (3)	dust, sea salt, black carbon (BC), primary organic carbon (OC), sulphate (and its gaseous precursors SO2 and DMS), biogenic secondary organic carbon from	BL mixing scheme based on Lock et al. (2000).	Diagnosed from stability profile (non-local scheme accounting for moist	Aerosols not modelled as separate species with fixed properties. Aerosol	Black carbon: 1.75 + 0.44i. Organic carbon and SOA: 1.5	Once organic carbon has mixed into a soluble mode it is assumed to be partial hygroscopic and takes up	BB aerosol emitted as hygrophobic (insoluble) primary aerosol

	oxidation of monoterpene.	Mass flux based on Gregory and Rowntree (1990), Derbyshire et al. (2011)	parcel ascent)	optical properties vary with the simulated composition, size distribution and water content.	+ 0i, sulphate 1.53 +1.e-7i, sea salt: 1.55 + 1.e-7i; dust: 1.53 + 0.0052i	approximately 40% of the water that the same mass of sulphate aerosol would take up in the model.	but can be coated with sulphate or mixed with other soluble modes. It then transfers to the accumulation soluble mode where it is assumed to be aged and partially hygroscopic. Typical lifetime in the (fresh) aitken insoluble mode is 2 days.
OsloCTM2	du, ss, OC, BC, sulfate, secondary organic aerosols (SOA), nitrate	Wet removal in grid boxes with convective precipitation from IFS (Bergle n et al., 2004)	PBL hight given in the IFS data.	All values in m2/g at 30% RH: Sulfate 3.70, BC fossil fuel external mixture 9.24, OC fossil fuel 4.92, BB(BC + OC) 5.04, nitrate 3.71, sea salt and mineral dust is size dependent	See Table 2 in (Myhre et al., 2007)	Based on (Magi and Hobbs, 2003) (1+1.31*(RH/100)^4.88)	80% of BC and 50% of OC are hydrophilic at the time of emissions. Aging time is dependent on season and latitude (Skeie et al., 2011)
SPRINTARS (5.5)	du, ss, OC, BC, sulfate (and its gaseous precursors SO_2 and DMS)	Takemura et al. (2000, 2002, 2005, 2009)	Takemura et al. (2000, 2002, 2005, 2009)	See (Takemura et al., 2002)	See (Takemura et al., 2002)	See (Takemura et al., 2002)	None

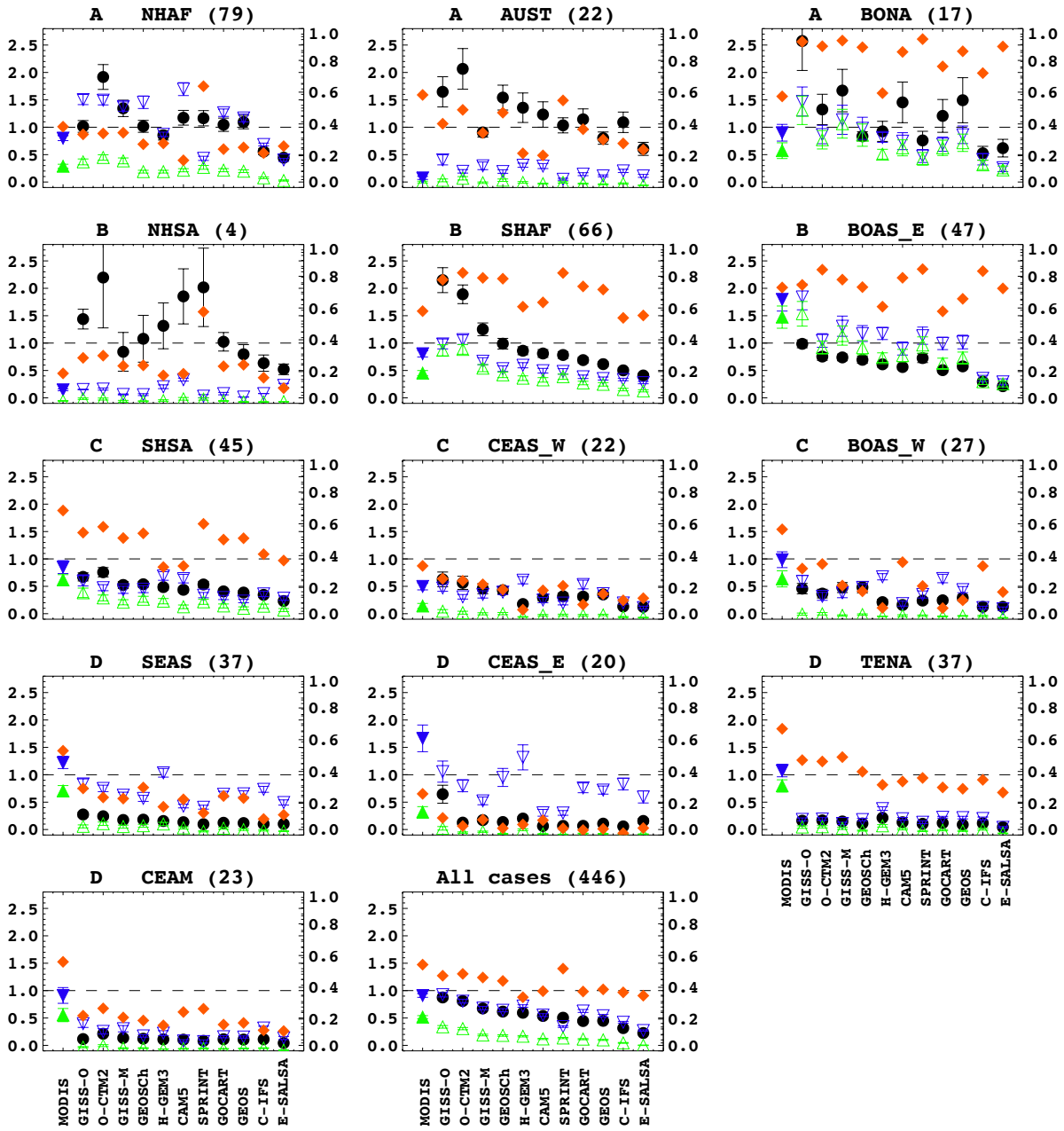

Figure S1 Ratios of model BB AOD to MODIS BB AOD (R_{BB_AOD}) for 11 models, aggregated over each of 13 regions (black dots and left Y axes), plus ratios when aggregated over all regions in the bottom row, right. Shown on the right Y axes are the mean model and MODIS total AOD (blue triangles) and BB AOD (green triangles) for all cases in the region, and the mean BB fraction of total AOD for each model in the region (red diamonds). The group identifiers defined in Section 3.1 are given in the upper left of each panel. Note that the models are ordered in these plots based on the overall R_{BB_AOD}, from highest to lowest, i.e., all individual case averages in a region were used to calculate one arithmetic mean for each model.

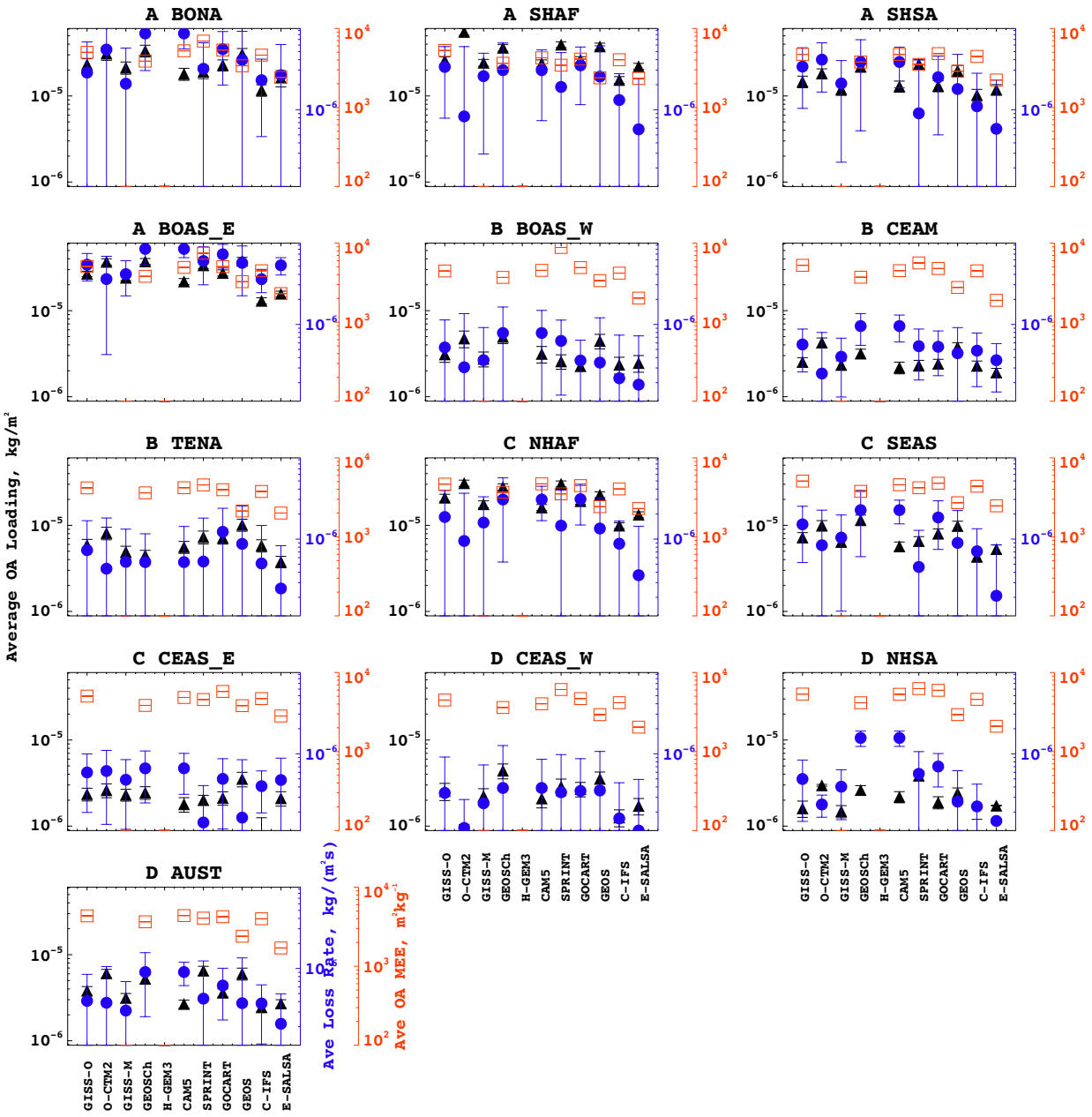

Figure S2 Plots showing the OA Mass Loading (kg/m^2; left Y axis and filled black triangles), OA Loss Frequency (s^{-1}; right blue Y axis and filled blue circles), and OA Mass Extinction Efficiency (m^2/kg; right orange Y axis and open orange squares) for 10 models in each of 13 region-specific panels. Note that Loss Frequency values are missing for the CAM5 model and MEEs are lacking for GISS-M and O-CTM2.

References

Andres, R. J. and Kasgnoc, a. D.: A time-averaged inventory of subaerial volcanic sulfur emissions, J. Geophys. Res., 103, 25251, https://doi.org/10.1029/98JD02091, 1998a.

Andres, R. J. and Kasgnoc, a. D.: A time-averaged inventory of subaerial volcanic sulfur emissions, J. Geophys. Res., 103, 25251, https://doi.org/10.1029/98JD02091, 1998b.

Bauer, S. E., Wright, D. L., Koch, D., Lewis, E. R., McGraw, R., Chang, L.-S., Schwartz, S. E., and Ruedy, R.: MATRIX (Multiconfiguration Aerosol TRacker of mIXing state): an aerosol microphysical module for global atmospheric models, Atmos Chem Phys, 8, 6003–6035, https://doi.org/10.5194/acp-8-6003-2008, 2008.

Bechtold, P., Semane, N., Lopez, P., Chaboureau, J.-P., Beljaars, A., and Bormann, N.: Representing Equilibrium and Nonequilibrium Convection in Large-Scale Models, J Atmos Sci, 71, 734–753, https://doi.org/10.1175/JAS-D-13-0163.1, 2014.

Berglen, T. F., Berntsen, T. K., Isaksen, I. S. A., and Sundet, J. K.: A global model of the coupled sulfur/oxidant chemistry in the troposphere: The sulfur cycle., J. Geophys. Res., 109, D19310, 2004.

Bergman, T., Kerminen, V. M., Korhonen, H., Lehtinen, K. J., Makkonen, R., Arola, A., Mielonen, T., Romakkaniemi, S., Kulmala, M., and Kokkola, H.: Evaluation of the sectional aerosol microphysics module SALSA implementation in ECHAM5-HAM aerosol-climate model, Geosci Model Dev, 5, 845–868, https://doi.org/10.5194/gmd-5-845-2012, 2012.

Bond, T. C., Bhardwaj, E., Dong, R., Jogani, R., Jung, S., Roden, C., Streets, D. G., and Trautmann, N. M.: Historical emissions of black and organic carbon aerosol from energy-related combustion, 1850-2000, Global Biogeochem Cycles, 21, https://doi.org/10.1029/2006GB002840, 2007.

Bouwman, A. F., Lee, D. S., Asman, W. A. H., Dentener, F. J., Van Der Hoek, K. W., and Olivier, J. G. J.: A global high-resolution emission inventory for ammonia, Global Biogeochem Cycles, 11, 561–587, https://doi.org/10.1029/97GB02266, 1997.

Bozzo, A., Benedetti, A., Flemming, J., Kipling, Z., and Rémy, S.: An aerosol climatology for global models based on the tropospheric aerosol scheme in the Integrated Forecasting System of ECMWF, Geosci Model Dev, 13, 1007–1034, https://doi.org/10.5194/gmd-13-1007-2020, 2020.

Carn, S. A., Fioletov, V. E., Mclinden, C. A., Li, C., and Krotkov, N. A.: A decade of global volcanic SO2emissions measured from space, Sci Rep, 7, 1–12, https://doi.org/10.1038/srep44095, 2017.

Chin, M., Ginoux, P., Kinne, S., Torres, O., Holben, B. N., Duncan, B. N., Martin, R. V, Logan, J. A., Higurashi, A., and Nakajima, T.: Tropospheric aerosol optical thickness from the GOCART model and comparisons with satellite and sun photometer measurements, J Atmos Sci, 59, 461–483, 2002.

Chin, M., Diehl, T., Dubovik, O., Eck, T. F., Holben, B. N., Sinyuk, A., and Streets, D. G.: Light absorption by pollution, dust, and biomass burning aerosols: a global model study and evaluation with AERONET measurements, Ann Geophys, 27, 3439–3464, https://doi.org/10.5194/angeo-27-3439-2009, 2009.

Dentener, F., Kinne, S., Bond, T., Boucher, O., Cofala, J., Generoso, S., Ginoux, P., Gong, S., Hoelzemann, J. J., Ito, A., Marelli, L., Penner, J. E., Putaud, J.-P., Textor, C., Schulz, M., van der Werf, G. R., and Wilson, J.: Emissions of primary aerosol and precursor gases in the years 2000 and 1750 prescribed data-sets for AeroCom, Atmos Chem Phys, 6, 4321–4344, 2006a.

Dentener, F., Drevet, J., Lamarque, J. F., Bey, I., Eickhout, B., Fiore, A. M., Hauglustaine, D., Horowitz, L. W., Krol, M., Kulshrestha, U. C., Lawrence, M., Galy-Lacaux, C., Rast, S., Shindell, D., Stevenson, D., Van Noije, T., Atherton, C., Bell, N., Bergman, D., Butler, T., Cofala, J., Collins, B., Doherty, R., Ellingsen, K., Galloway, J., Gauss, M., Montanaro, V., Müller, J. F., Pitari, G., Rodriguez, J., Sanderson, M., Solmon, F., Strahan, S., Schultz, M., Sudo, K., Szopa, S., and Wild, O.: Nitrogen and sulfur deposition on regional and global scales: A multimodel evaluation, Global Biogeochem Cycles, 20, https://doi.org/10.1029/2005GB002672, 2006b.

Derbyshire, S. H., Maidens, A. V., Milton, S. F., Stratton, R. A., and Willett, M. R.: Adaptive detrainment in a convective parametrization, Quarterly Journal of the Royal Meteorological Society, 137, 1856–1871, https://doi.org/10.1002/qj.875, 2011.

Diehl, T., Heil, A., Chin, M., Pan, X., Streets, D., Schultz, M., and Kinne, S.: Anthropogenic, biomass burning, and volcanic emissions of black carbon, organic carbon, and SO2 from 1980 to 2010 for hindcast model experiments, Atmospheric Chemistry and Physics Discussion, 12, 24895–24954, https://doi.org/10.5194/acpd-12-24895-2012, 2012.

Duncan Fairlie, T., Jacob, D. J., and Park, R. J.: The impact of transpacific transport of mineral dust in the United States, Atmos Environ, 41, 1251–1266, https://doi.org/10.1016/j.atmosenv.2006.09.048, 2007.

Fisher, J. A., Jacob, D. J., Wang, Q., Bahreini, R., Carouge, C. C., Cubison, M. J., Dibb, J. E., Diehl, T., Jimenez, J. L., Leibensperger, E. M., Lu, Z., Meinders, M. B. J., Pye, H. O. T., Quinn, P. K., Sharma, S., Streets, D. G., van Donkelaar, A., and Yantosca, R. M.: Sources, distribution, and acidity of sulfate-ammonium aerosol in the Arctic in winter-spring, Atmos Environ, 45, 7301–7318, https://doi.org/10.1016/j.atmosenv.2011.08.030, 2011.

Ghan, S. J. and Zaveri, R. A.: Parameterization of optical properties for hydrated internally mixed aerosol, Journal of Geophysical Research Atmospheres, 112, https://doi.org/10.1029/2006JD007927, 2007.

Ginoux, P., Chin, M., Tegen, I., Prospero, J. M., Holben, B., Dubovik, O., and Lin, S.-J.: Sources and distributions of dust aerosols simulated with the GOCART model, J Geophys Res, 106, 20255–20274, https://doi.org/10.1029/2000JD000053, 2001.

Gong, S. L.: A parameterization of sea-salt aerosol source function for sub- and super-micron particles, Global Biogeochem Cycles, 17, n/a-n/a, https://doi.org/10.1029/2003GB002079, 2003.

Gregory, D. and Rowntree, P. R.: A Mass Flux Convection Scheme with Representation of Cloud Ensemble Characteristics and Stability-Dependent Closure, Mon Weather Rev, 118, 1483–1506, https://doi.org/10.1175/1520-0493(1990)118<1483:AMFCSW>2.0.CO;2, 1990.

Grini, A., Korhonen, H., Lehtinen, K. E. J., Isaksen, I. S. A., and Kulmala, M.: A combined photochemistry/aerosol dynamics model: model development and a study of new particle formation, Boreal Env Res, 10, 525–541, 2005.

Hess, M., Koepke, P., and Schult, I.: Optical Properties of Aerosols and Clouds: The Software Package OPAC, Bull Am Meteorol Soc, 79, 831–844, https://doi.org/10.1175/1520-0477(1998)079<0831:OPOAAC>2.0.CO;2, 1998.

Holtslag, A. A. M. and Boville, B. A.: Local versus nonlocal boundary-layer diffusion in a global climate model, J Clim, 6, 1825–1842, https://doi.org/10.1175/1520-0442(1993)006<1825:LVNBLD>2.0.CO;2, 1993.

Hu, W. W., Campuzano-Jost, P., Palm, B. B., Day, D. A., Ortega, A. M., Hayes, P. L., Krechmer, J. E., Chen, Q., Kuwata, M., Liu, Y. J., De Sá, S. S., McKinney, K., Martin, S. T., Hu, M., Budisulistiorini, S. H., Riva, M., Surratt, J. D., St. Clair, J. M., Isaacman-Van Wertz, G., Yee, L. D., Goldstein, A. H., Carbone, S., Brito, J., Artaxo, P., De Gouw, J. A., Koss, A., Wisthaler, A., Mikoviny, T., Karl, T., Kaser, L., Jud, W., Hansel, A., Docherty, K. S., Alexander, M. L., Robinson, N. H., Coe, H., Allan, J. D., Canagaratna, M. R., Paulot, F., and Jimenez, J. L.: Characterization of a real-time tracer for isoprene epoxydiols-derived secondary organic aerosol (IEPOX-SOA) from aerosol mass spectrometer measurements, Atmos Chem Phys, 15, 11807–11833, https://doi.org/10.5194/acp-15-11807-2015, 2015.

Jacobson, M. Z.: Fundamentals of Atmospheric Modeling, Second edi., Cambridge University Press, New York, 2005.

Jaeglé, L., Quinn, P. K., Bates, T. S., Alexander, B., and Lin, J. T.: Global distribution of sea salt aerosols: New constraints from in situ and remote sensing observations, Atmos Chem Phys, 11, 3137–3157, https://doi.org/10.5194/acp-11-3137-2011, 2011.

Kaiser, J. W., Heil, A., Andreae, M. O., Benedetti, A., Chubarova, N., Jones, L., Morcrette, J.-J., Razinger, M., Schultz, M. G., Suttie, M., van der Werf, G. R., Werf, G. R. van der, and van der Werf, G. R.: Biomass burning emissions estimated with a global fire assimilation system based on observed fire radiative power, Biogeosciences, 9, 527–554, https://doi.org/doi:10.5194/bg-9-527-2012, 2012.

Kim, D., Chin, M., Bian, H., Tan, Q., Brown, M. E., Zheng, T., You, R., Diehl, T., Ginoux, P., and Kucsera, T.: The effect of the dynamic surface bareness on dust source function, emission, and distribution, Journal of Geophysical Research Atmospheres, 118, 871–886, https://doi.org/10.1029/2012JD017907, 2013.

Lamarque, J. F., Bond, T. C., Eyring, V., Granier, C., Heil, A., Klimont, Z., Lee, D., Liousse, C., Mieville, A., Owen, B., Schultz, M. G., Shindell, D., Smith, S. J., Stehfest, E., Van Aardenne, J., Cooper, O. R., Kainuma, M., Mahowald, N., McConnell, J. R., Naik, V., Riahi, K., and van Vuuren, D. P.: Historical (1850–2000) gridded anthropogenic and biomass burning emissions of reactive gases and aerosols: methodology and application, Atmos. Chem. Phys., 10, 7017–7039, https://doi.org/10.5194/acp-10-7017-2010, 2010.

Lin, J. T. and McElroy, M. B.: Impacts of boundary layer mixing on pollutant vertical profiles in the lower troposphere: Implications to satellite remote sensing, Atmos Environ, 44, 1726–1739, https://doi.org/10.1016/j.atmosenv.2010.02.009, 2010.

Lin, J. T., Youn, D., Liang, X. Z., and Wuebbles, D. J.: Global model simulation of summertime U.S. ozone diurnal cycle and its sensitivity to PBL mixing, spatial resolution, and emissions, Atmos Environ, 42, 8470–8483, https://doi.org/10.1016/j.atmosenv.2008.08.012, 2008.

Lock, A. P., Brown, A. R., Bush, M. R., Martin, G. M., and Smith, R. N. B.: A New Boundary Layer Mixing Scheme. Part I: Scheme Description and Single-Column Model Tests, Mon Weather Rev, 128, 3187–3199, https://doi.org/10.1175/1520-0493(2000)128<3187:ANBLMS>2.0.CO;2, 2000.

Magi, B. I. and Hobbs, P. V.: Effects of humidity on aerosols in southern Africa during the biomass burning season, Journal of Geophysical Research: Atmospheres, 108, n/a-n/a, https://doi.org/10.1029/2002JD002144, 2003.

McGrath-Spangler, E. L. and Molod, A.: Comparison of GEOS-5 AGCM planetary boundary layer depths computed with various definitions, Atmos Chem Phys, 14, 6717–6727, https://doi.org/10.5194/acp-14-6717-2014, 2014.

Monahan, E. C. and O'Muircheartaigh, I. G.: Whitecaps and the passive remote sensing of the ocean surface, Int J Remote Sens, 7, 627–642, https://doi.org/10.1080/01431168608954716, 1986.

Moorthi, S. and Suarez, M. J.: Relaxed Arakawa-Schubert. A Parameterization of Moist Convection for General Circulation Models, Mon Weather Rev, 120, 978–1002, https://doi.org/10.1175/1520-0493(1992)120<0978:RASAPO>2.0.CO;2, 1992.

Morcrette, J.-J., Boucher, O., Jones, L., Salmond, D., Bechtold, P., Beljaars, A., Benedetti, A., Bonet, A., Kaiser, J. W., Razinger, M., Schulz, M., Serrar, S., Simmons, A. J., Sofiev, M., Suttie, M., Tompkins, A. M., and Untch, A.: Aerosol analysis and forecast in the European Centre for Medium-Range Weather Forecasts Integrated Forecast System: Forward modeling, J Geophys Res, 114, D06206, https://doi.org/10.1029/2008JD011235, 2009.

Myhre, G., Bellouin, N., Berglen, T. F., Berntsen, T. K., Boucher, O., Grini, A., Isaksen, I. S. A., Johnsrud, M., Mishchenko, M. I., Stordal, F., and Tanré, D.: Comparison of the radiative properties and direct radiative effect of aerosols from a global aerosol model and remote sensing data over ocean, Tellus B Chem Phys Meteorol, 59, 115–129, https://doi.org/10.1111/j.1600-0889.2006.00226.x, 2007.

Nordeng, T. E.: Extended versions of the convective parametrization scheme at ECMWF and their impact on the mean and transient activity of the model in the tropics, Technical Memorandum, 1–41, 1994.

Olivier, J. G. J., Van Aardenne, J. A., Dentener, F. J., Pagliari, V., Ganzeveld, L. N., and Peters, J. A. H. W.: Recent trends in global greenhouse gas emissions:regional trends 1970–2000 and spatial

distributionof key sources in 2000, Environ Sci (Ruse), 2, 81–99, https://doi.org/10.1080/15693430500400345, 2005.
Park, S. and Bretherton, C. S.: The University of Washington shallow convection and moist turbulence schemes and their impact on climate simulations with the community atmosphere model, J Clim, 22, 3449–3469, https://doi.org/10.1175/2008JCLI2557.1, 2009.
Paugam, R., Wooster, M., Atherton, J., Freitas, S. R., Schultz, M. G., and Kaiser, J. W.: Development and optimization of a wildfire plume rise model based on remote sensing data inputs – Part 2, Atmospheric Chemistry and Physics Discussions, 15, 9815–9895, https://doi.org/10.5194/acpd-15-9815-2015, 2015.
Rémy, S., Kipling, Z., Flemming, J., Boucher, O., Nabat, P., Michou, M., Bozzo, A., Ades, M., Huijnen, V., Benedetti, A., Engelen, R., Peuch, V.-H., and Morcrette, J.-J.: Description and evaluation of the tropospheric aerosol scheme in the European Centre for Medium-Range Weather Forecasts (ECMWF) Integrated Forecasting System (IFS-AER, cycle 45R1), Geosci Model Dev, 12, 4627–4659, https://doi.org/10.5194/gmd-12-4627-2019, 2019.
Schmidt, G. A., Kelley, M., Nazarenko, L., Ruedy, R., Russell, G. L., Aleinov, I., Bauer, M., Bauer, S. E., Bhat, M. K., Bleck, R., Canuto, V., Chen, Y.-H., Cheng, Y., Clune, T. L., Del Genio, A., de Fainchtein, R., Faluvegi, G., Hansen, J. E., Healy, R. J., Kiang, N. Y., Koch, D., Lacis, A. A., LeGrande, A. N., Lerner, J., Lo, K. K., Matthews, E. E., Menon, S., Miller, R. L., Oinas, V., Oloso, A. O., Perlwitz, J. P., Puma, M. J., Putman, W. M., Rind, D., Romanou, A., Sato, M., Shindell, D. T., Sun, S., Syed, R. A., Tausnev, N., Tsigaridis, K., Unger, N., Voulgarakis, A., Yao, M.-S., and Zhang, J.: Configuration and assessment of the GISS ModelE2 contributions to the CMIP5 archive, J Adv Model Earth Syst, 6, 141–184, https://doi.org/https://doi.org/10.1002/2013MS000265, 2014.
Skeie, R. B., Berntsen, T., Myhre, G., Pedersen, C. A., Strãm, J., Gerland, S., and Ogren, J. A.: Black carbon in the atmosphere and snow, from pre-industrial times until present, Atmos Chem Phys, 11, 6809–6836, https://doi.org/10.5194/acp-11-6809-2011, 2011.
Spracklen, D. V, Pringle, K. J., Carslaw, K. S., Chipperfield, M. P., and Mann, G. W.: A global off-line model of size-resolved aerosol microphysics: I. Model development and prediction of aerosol properties, Atmos Chem Phys, 5, 2227–2252, https://doi.org/10.5194/acp-5-2227-2005, 2005.
Stettler, M. E. J., Eastham, S., and Barrett, S. R. H.: Air quality and public health impacts of UK airports. Part I: Emissions, Atmos Environ, 45, 5415–5424, https://doi.org/10.1016/j.atmosenv.2011.07.012, 2011.
Stevens, B., Giorgetta, M., Esch, M., Mauritsen, T., Crueger, T., Rast, S., Salzmann, M., Schmidt, H., Bader, J., Block, K., Brokopf, R., Fast, I., Kinne, S., Kornblueh, L., Lohmann, U., Pincus, R., Reichler, T., and Roeckner, E.: Atmospheric component of the MPI-M earth system model: ECHAM6, J Adv Model Earth Syst, 5, 146–172, https://doi.org/10.1002/jame.20015, 2013.
Stohl, A., Aamaas, B., Amann, M., Baker, L. H., Bellouin, N., Berntsen, T. K., Boucher, O., Cherian, R., Collins, W., Daskalakis, N., Dusinska, M., Eckhardt, S., Fuglestvedt, J. S., Harju, M., Heyes, C., Hodnebrog, Hao, J., Im, U., Kanakidou, M., Klimont, Z., Kupiainen, K., Law, K. S., Lund, M. T., Maas, R., MacIntosh, C. R., Myhre, G., Myriokefalitakis, S., Olivié, D., Quaas, J., Quennehen, B., Raut, J. C., Rumbold, S. T., Samset, B. H., Schulz, M., Seland, Shine, K. P., Skeie, R. B., Wang, S., Yttri, K. E., and Zhu, T.: Evaluating the climate and air quality impacts of short-lived pollutants, Atmos Chem Phys, 15, 10529–10566, https://doi.org/10.5194/acp-15-10529-2015, 2015.
Streets, D. G., Zhang, Q., Wang, L., He, K., Hao, J., Wu, Y., Tang, Y., and Carmichael, G. R.: Revisiting China's CO emissions after the Transport and Chemical Evolution over the Pacific (TRACE-P) mission: Synthesis of inventories, atmospheric modeling, and observations, Journal of Geophysical Research Atmospheres, 111, https://doi.org/10.1029/2006JD007118, 2006.
Takemura, T., Okamoto, H., Maruyama, Y., Numaguti, A., Higurashi, A., and Nakajima, T.: Global three-dimensional simulation of aerosol optical thickness distribution of various origins, Journal of

Geophysical Research: Atmospheres, 105, 17853–17873, https://doi.org/10.1029/2000JD900265, 2000.
Takemura, T., Nakajima, T., Dubovik, O., Holben, B. N., and Kinne, S.: Single-scattering albedo and radiative forcing of various aerosol species with a global three-dimensional model, J Clim, 15, 333–352, https://doi.org/10.1175/1520-0442(2002)015<0333:SSAARF>2.0.CO;2, 2002.
Takemura, T., Nozawa, T., Emori, S., Nakajima, T. Y., and Nakajima, T.: Simulation of climate response to aerosol direct and indirect effects with aerosol transport-radiation model, Journal of Geophysical Research D: Atmospheres, 110, 1–16, https://doi.org/10.1029/2004JD005029, 2005.
Takemura, T., Egashira, M., Matsuzawa, K., Ichijo, H., O'Ishi, R., and Abe-Ouchi, A.: A simulation of the global distribution and radiative forcing of soil dust aerosols at the Last Glacial Maximum, Atmos Chem Phys, 9, 3061–3073, https://doi.org/10.5194/acp-9-3061-2009, 2009.
Tegen, I., Harrison, S. P., Kohfeld, K., Prentice, I. C., Coe, M., and Heimann, M.: Impact of vegetation and preferential source areas on global dust aerosol: Results from a model study, Journal of Geophysical Research Atmospheres, 107, https://doi.org/10.1029/2001JD000963, 2002.
Tiedtke, M.: A Comprehensive Mass Flux Scheme for Cumulus Parameterization in Large-Scale Models, Mon Weather Rev, 117, 1779–1800, https://doi.org/10.1175/1520-0493(1989)117<1779:ACMFSF>2.0.CO;2, 1989.
Troen, I. B. and Mahrt, L.: A simple model of the atmospheric boundary layer; sensitivity to surface evaporation, Boundary Layer Meteorol, 37, 129–148, https://doi.org/10.1007/BF00122760, 1986.
Wesely, M. L.: Parameterization of surface resistances to gaseous dry deposition in regional-scale numerical models, Atmospheric Environment (1967), 23, 1293–1304, https://doi.org/https://doi.org/10.1016/0004-6981(89)90153-4, 1989.
Woodward, S.: Modeling the atmospheric life cycle and radiative impact of mineral dust in the Hadley Centre climate model, Journal of Geophysical Research: Atmospheres, 106, 18155–18166, https://doi.org/10.1029/2000JD900795, 2001.
Xiao, Y., Logan, J. A., Jacob, D. J., Hudman, R. C., Yantosca, R., and Blake, D. R.: Global budget of ethane and regional constraints on U.S. sources, Journal of Geophysical Research Atmospheres, 113, https://doi.org/10.1029/2007JD009415, 2008.
Yevich, R. and Logan, J. A.: An assessment of biofuel use and burning of agricultural waste in the developing world, Global Biogeochem Cycles, 17, n/a-n/a, https://doi.org/10.1029/2002GB001952, 2003.
Zhang, G. J. and McFarlane, N. A.: Sensitivity of climate simulations to the parameterization of cumulus convection in the canadian climate centre general circulation model, Atmosphere - Ocean, 33, 407–446, https://doi.org/10.1080/07055900.1995.9649539, 1995.
Zhang, Q., Streets, D. G., Carmichael, G. R., He, K. B., Huo, H., Kannari, A., Klimont, Z., Park, I. S., Reddy, S., Fu, J. S., Chen, D., Duan, L., Lei, Y., Wang, L. T., and Yao, Z. L.: Asian emissions in 2006 for the NASA INTEX-B mission, Atmos Chem Phys, 9, 5131–5153, https://doi.org/10.5194/acp-9-5131-2009, 2009.